

RESEARCH ARTICLE OPEN ACCESS

A Systematic Study on the Polymerization Processes and Resulting Polymer Properties of Bioinspired Sesamol and Diamine-Based Benzoxazines

Thorben S. Haubold^{1,2} | Gideon Abels¹ | Katharina Koschek¹ 

¹Fraunhofer Institute for Manufacturing Technology and Advanced Materials IFAM, Bremen, Germany | ²Department 2 Biology/Chemistry, University of Bremen, Bremen, Germany

Correspondence: Katharina Koschek (katharina.koschek@ifam.fraunhofer.de)

Received: 16 July 2024 | **Revised:** 7 October 2024 | **Accepted:** 27 October 2024

Funding: This work was supported by BMWK (03SX515E).

Keywords: benzoxazines | diamines | polybenzoxazines | sesamol | thermoset

ABSTRACT

Benzoxazine monomers based on sesamol and aliphatic diamines with a systematic variation of chain lengths were synthesized to study the influence of the diamine chain lengths on thermal and thermo-mechanical properties. Differential scanning calorimetry analysis revealed an even-odd effect as the melting point for monomers with an odd chain length was at least 35°C lower compared to their even counterparts. In addition, longer diamine chain lengths increased the beginning of the polymerization from 187°C for diaminoethane (DAE) up to 218°C for diaminohexane (DAH). Rheological analysis revealed a short time frame between the melting and polymerization for monomers based on diaminoethane, -propane or -butane preventing a polymerization. Polymerization was successful for sesamol benzoxazine with diaminopentane (S-DAPe) and -hexane (S-DAH) resulting polymers with high glass transition temperatures of up to 228°C for poly(S-DAPe) and 231°C for poly(S-DAH), respectively. Remarkably, it was found that S-DAH could also be polymerized at a lower temperature of 155°C yielding a T_g of 175°C. Furthermore, MCC results showed that peak heat release rate and total heat release of the diamine based polybenzoxazines decrease with decreasing chain length. In comparison to other sesamol based benzoxazines the presence of diamine linkers result in bisbenzoxazines with higher T_g .

1 | Introduction

Polybenzoxazines as promising phenolic type thermosets feature outstanding properties such as near zero-volume shrinkage upon polymerization [1], high glass transition temperatures [2], good mechanical properties [2, 3], and a good initial flame retardancy [4]. The combination of the phenolic structure as well as the intra- and intermolecular hydrogen bonds is responsible for polybenzoxazines thermal and thermo-mechanical properties. A suitable combination of phenols and amines promoting H-bonds can further improve the overall properties. Additionally, the high flexibility in molecular design allows for substitution

of mainly fossil based phenols, amines, and aldehydes against biobased analogues. Among others, cardanol [5–7], guaiacol [8, 9], magnolol [10], eugenol [11], phloretic acid [12, 13], and sesamol [14] were previously described as phenolic component, furfurylamine [14, 15], stearylamine [15], chitosan [16] or isomannide [17] as the amine and benzaldehyde [18] or furfural [19] as aldehyde. A detailed review about biobased benzoxazines was published by Lyu and Ishida [20].

In recent years, sesamol has drawn increasing interest as a biobased building block for benzoxazine synthesis in particular if high thermal stability is required for potential use in high

This is an open access article under the terms of the [Creative Commons Attribution](https://creativecommons.org/licenses/by/4.0/) License, which permits use, distribution and reproduction in any medium, provided the original work is properly cited.

© 2024 The Author(s). *Journal of Applied Polymer Science* published by Wiley Periodicals LLC.

performance applications. Salum et al. combined sesamol with furfurylamine and paraformaldehyde to obtain a monofunctional benzoxazine monomer with a low T_m , high thermal stability and high char yield [14]. In a following attempt Machado et al. substituted paraformaldehyde by 4-hydroxybenzaldehyde in order to further increase the thermal stability and the biobased content. The resulting benzoxazine monomer exhibited a high T_m of 190°C, a higher thermal stability and a lower heat release capacity [21]. Liu et al. combined sesamol with the diterpene amine dehydroabietylamine and stearylamine, respectively. The resulting polybenzoxazines have been studied as coatings and showed good corrosion resistance [22]. Parallel to this work, Necolau et al. used polyethyleneimine and diamines to synthesize a multifunctional sesamol based benzoxazine monomer, respectively [23].

Among the previously described amines, diamines allow the formation of bisbenzoxazines. Polybenzoxazines based on bisbenzoxazines exhibit a higher crosslinking density in comparison to monofunctional amines and by this, higher thermo-mechanical properties [2]. Allen and Ishida revealed that the use of a short chained aliphatic diamine like putrescine or diaminohexane in combination with either phenol or guaiacol lead to similar thermal stability and thermo-mechanical properties as for the conventional bisphenol A and aniline based benzoxazine [31]. Moreover, Putrescine can be obtained from renewable feedstock (glucose) combined with an engineered strain of *Escherichia coli* [24] whereas diaminohexane results from a biosynthesis patented by Covestro and Genomatica [25]. Another potential diamine similar to diaminohexane is cadaverine, as short-chained pentyl diamine with an odd chain length. It is derived from the decarboxylation of lysine [26].

Thus, the state of the art indicates that sesamol and diamines are promising biobased reactants for the design of benzoxazines with good mechanical and thermal properties. Additionally, Bunn described that the use of different even-odd numbered aliphatic diamines can be used to adjust the T_m of monomers and polymers (e.g., for polyurethanes) [27]. Considering the high melting temperatures of benzoxazines, the marginal structural difference between cadaverine and diaminohexane might have a significant impact on the thermal properties and subsequently on the manufacturing possibilities of benzoxazines synthesized from these amines. Therefore, the objective in the present work was the synthesis and systematic study of thermally stable biobased bisbenzoxazine monomers and the resulting polymers using sesamol and aliphatic diamines with varying chain lengths ranging from two to six methylene groups (Scheme 1). A monofunctional sesamol-furfurylamine based benzoxazine was used as reference. The polymerization was investigated in dependence of application of pressure, different curing times and the use of an initiator. Furthermore, thermal characteristics of

the monomers as well as the thermal and mechanical properties and the combustion behavior of the resulting polymers were analyzed and correlated with the molecular structure and polymerization conditions.

2 | Results and Discussion

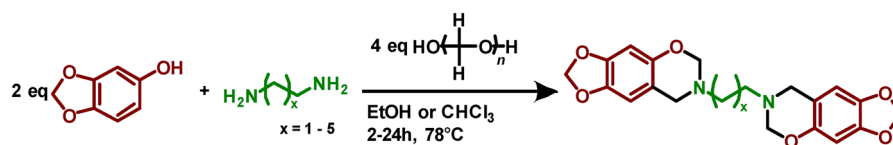
2.1 | Synthesis and Characterization of Sesamol-Based Monomers

The bifunctional benzoxazine monomers S-DAE, S-DAPr, S-DAB, S-DAPE, and S-DAH were obtained from sesamol, the corresponding aliphatic diamines DAE, DAPr, DAB, DAPE, and DAH and paraformaldehyde. Benzoxazine monomer syntheses were performed in ethanol as green solvent except for S-DAPr which was synthesized in chloroform. All resulting monomer structures were confirmed by FT-IR, ^1H NMR, ^{13}C NMR, and high-resolution mass spectrometry (HR-MS).

Nuclear magnetic resonance (NMR) spectra of all benzoxazine monomers showed two oxazine related singlets at 4.76 ppm and 3.87 ppm corresponding to $\text{O}-\text{CH}_2-\text{N}$ (B) and $\text{Ar}-\text{CH}_2-\text{N}$ (C) protons in case of S-DAPr, S-DAB, S-DAPE, and S-DAH and at 4.81 ppm and 3.93 ppm in case of S-DAE (Figure 1). These signals confirmed the formation of the respective benzoxazine rings. The chemical shift for S-DAE resulted from the short aliphatic chain length and a subsequent mutual effect of the adjacent oxazine units.

The signals of the diamine methylene groups (L) were low-field shifted with decreasing amine chain length from 2.70 ppm for S-DAH/DAPE to 2.73, 2.78, and 2.94 ppm for S-DAB, S-DAPr, and S-DAE, respectively. The $\text{N}-\text{CH}_2-\text{CH}_2$ methylene groups (M) were also low field shifted with shorter chain lengths, accordingly. The corresponding proton signals were between 1.54 and 1.58 ppm for S-DAH, S-DAPE, and S-DAB and at 1.78 ppm for S-DAPr, respectively. S-DAPE and S-DAH further showed proton signals of the $\text{N}-(\text{CH}_2)_2-\text{CH}_2-$ methylene group at 1.37 and 1.35 ppm, respectively.

In addition, all monomers exhibited a singlet proton signal in the low-field region at 5.86 ppm that is assigned to the $\text{O}-\text{CH}_2-\text{O}$ methylene group (A) of the acetyl group. The two singlet protons in the aromatic region at 6.33 ppm and 6.40 ppm indicated that only the proposed isomeric structure (Figure 1), which is in *meta* position regarding the methylenedioxy group, was formed as reported for different sesamol and amine based benzoxazines [14]. A benzoxazine in *ortho* position regarding the methylenedioxy group would exhibit two doublet signals for the aromatic region. The absence of any proton signal in the region of 3.7 ppm, which is typical for ring-opened methylene groups in benzoxazine oligomers,



SCHEME 1 | Reaction scheme of sesamol, diamines with different chain lengths and paraformaldehyde in ethanol or chloroform. [Color figure can be viewed at [wileyonlinelibrary.com](https://onlinelibrary.wiley.com)]

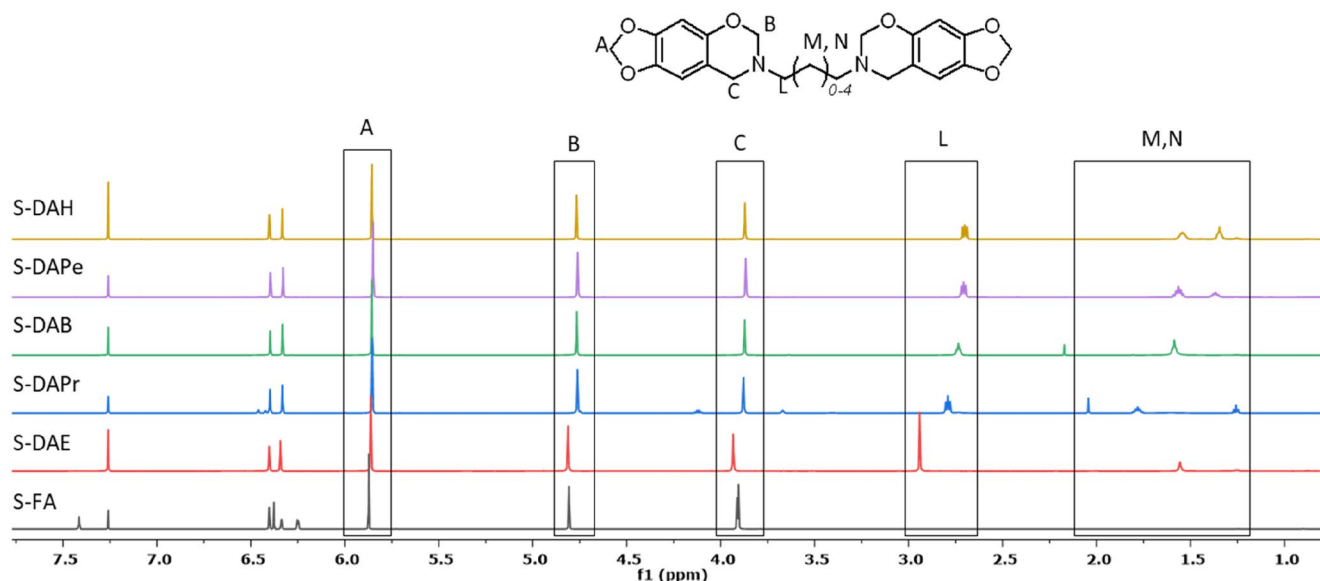


FIGURE 1 | ^1H NMR of different sesamol and aliphatic diamine-based benzoxazine monomers. [Color figure can be viewed at [wileyonlinelibrary.com](https://onlinelibrary.wiley.com)]

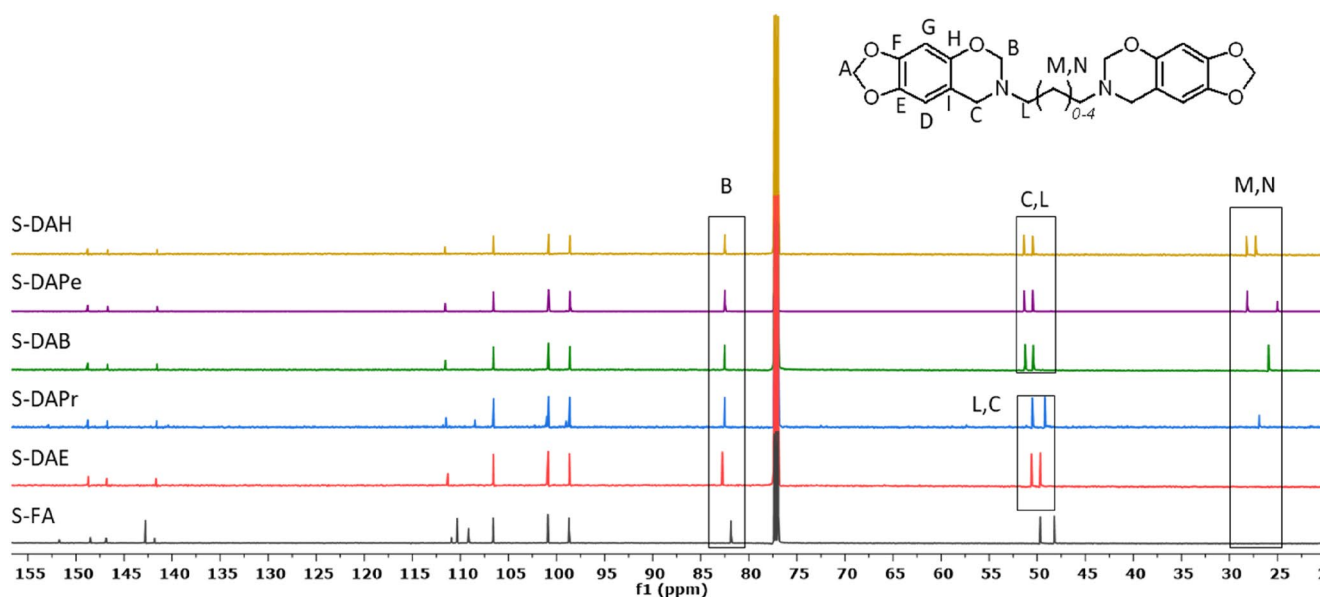


FIGURE 2 | ^{13}C NMR analysis of sesamol and different aliphatic diamine-based benzoxazines. [Color figure can be viewed at [wileyonlinelibrary.com](https://onlinelibrary.wiley.com)]

further indicated that the precipitation and washing with ethanol successfully removed any oligomeric material. This is important for the investigation of polymerization behavior.

The monomers were also characterized by ^{13}C NMR spectroscopy (Figure 2). All monomers revealed the same pattern in the aromatic region from 99 to 149 ppm without a distinguishable difference. Peaks at 82 ppm and 50 ppm corresponded to the benzoxazine typical $\text{O}-\text{CH}_2-\text{N}$ and the $\text{Ar}-\text{CH}_2-\text{N}$ groups, respectively. The aliphatic $\text{N}-\text{CH}_2-\text{CH}_2$ group (L) was at 51 ppm for S-DAB, S-DAPe, and S-DAH. For S-DAE and S-DAPr, the methylene signals were shifted to 49 ppm due to the decreasing amine chain length as described for the ^1H NMR spectra. Further ^{13}C NMR signals of the aliphatic moiety (M, N) were observed between 25 and 30 ppm.

FT-IR spectra were recorded to confirm monomer specific functional groups. All five sesamol based monomers exhibited almost identical spectra (Figure S1) showing typical benzoxazine bands at 1440, 1395, and 1188 cm^{-1} corresponding to CH_2 bending, $\text{C}-\text{N}-\text{C}$ asymmetric stretching and $\text{H}-\text{C}-\text{O}-\text{C}$ torsion in the oxazine ring, respectively. The absorption at 1475 cm^{-1} was assigned to the distinctive methylenedioxybenzene motif of sesamol and the one at 875 cm^{-1} to the out-of-plane bond for tetra-substituted benzene resulting from the benzoxazine formation. In the region between 890 and 960 cm^{-1} as well as between 1060 and 1020 cm^{-1} symmetric and asymmetric $\text{C}-\text{O}$ stretching modes of the sesamol moiety and the benzoxazine ring are overlapping. The introduced aliphatic linker varying in chain length did not impact FT-IR absorption of the resulting sesamol based bifunctional benzoxazine monomers.

2.2 | Impact of the Linker Chain Length on Thermal Properties

2.2.1 | Monomer Related Properties

The influence of the linker chain length on the melting point (T_m), the onset temperature of the ring-opening polymerization (ROP) (T_{onset}) and the molar polymerization enthalpy (ΔH_M) of the bifunctional benzoxazines was investigated by differential scanning calorimetry (DSC) (Figures 3, S2, and Table 1). Most bifunctional benzoxazines exhibited higher T_m in comparison to the monofunctional benzoxazine based on sesamol and furfurylamine (S-FA) except for S-DAPe. The T_m differed strongly but showed a pattern depending on the parity of the chain length. Bisbenzoxazines with even numbered linkers such as in S-DAE ($T_m = 176^\circ\text{C}$) and S-DAB ($T_m = 186^\circ\text{C}$) had exceptionally high T_m compared to odd numbered linkers such as in S-DAPr ($T_m = 139^\circ\text{C}$) and S-DAPe ($T_m = 98$) (Figure 3a). An increasing T_m for S-DAB in comparison to S-DAE was in accordance with findings from Necolau et al. [23] S-DAH ($T_m = 141^\circ\text{C}$) exhibited a higher T_m than S-DAPe and therefore followed the parity pattern as well. The observations indicated that the number of methylene groups affected the structure and by this the phase transition temperatures. Furthermore, the effect showed a parity dependency within the investigated number of methylene groups. It is assumed that the reduced symmetry for molecules with an odd number of methylene groups affects T_m . Alternations of T_m with aliphatic chains are known in literature [28] and were reported for other polymers such as polycarbonates and polyesters [29, 30].

Complementary to DSC, rheological analyses were performed to investigate the temperature of the polymerization begin (T_{onset}). DSC analysis revealed a T_{onset} of 187°C for S-DAE, which increased with longer chain lengths to 218°C for S-DAH. Hereby, no parity was observed for monomers with an even and odd number of methylene groups (Figures 4, S3, and Table 1). For rheological analysis, a value of 15 Pas was set as the polymerization begin due to its distinct difference from the fluctuating baseline. The measured T_{onset} 's were at 175°C ,

185°C , 195°C , 200°C , 210°C , and 230°C for S-DAPr, S-DAE, S-DAPe, S-DAB, S-DAH, and S-FA, respectively and showed a clear dependence on the amine chain length and also indicated that monomers with an odd-chain length polymerize sooner than even counterparts. However, the observed tendency differed compared to the T_{onset} determined from the DSC data, where only a shift based on the chain length was found and no even-odd effect. The different tendency from rheological analysis may be a result based on their molecular polymerization enthalpy (ΔH_M), as 197, 180, 176, 155, 152, and 58 kJ/mol for S-DAPr, S-DAE, S-DAPe, S-DAB, S-DAH, and S-FA were observed. Thus, monomers with a higher ΔH_M self-catalyze their own polymerization in an autocatalytic way, polymerizing faster in a rheological experiment compared to DSC because of the larger sample mass. As a result, a parity pattern for the ROP was observed for T_{onset} for rheological analysis compared to the DSC results, as the odd methylene-numbered S-DAPr and S-DAPe polymerize faster than those with even methylene-groups like S-DAE and S-DAB.

Overall, T_{onset} increased for the even- and odd-systems, respectively, in both DSC and rheological measurements, while a general increase from S-DAE to S-DAH was found only for the DSC analysis. This general increase of T_{onset} with longer aliphatic chain length matched literature reports, in which an increasing chain length led to a slower polymerization process [31, 32]. Interestingly, for the rheological analysis the lower polymerization onset of odd-chain lengths seemingly deviated from the literature reports which was also seen for T_m . However, Allen et al. only used even chain lengths so it is possible that a similar effect would have been found with odd chain lengths.

Thermogravimetric analysis (TGA) was used to determine the thermal stability of the monomers under both nitrogen and ambient atmosphere (Table S1 and Figure S4). The initial degradation temperature ($T_{5\%}$) for all diamine-based monomers was between 182°C for S-DAPr and 191°C and S-DAH, with no clear dependency on the chain length and parity pattern. Changes between ambient and nitrogen atmosphere did not result in a difference for $T_{5\%}$. The $T_{5\%}$ and also the $T_{10\%}$ of the bifunctional

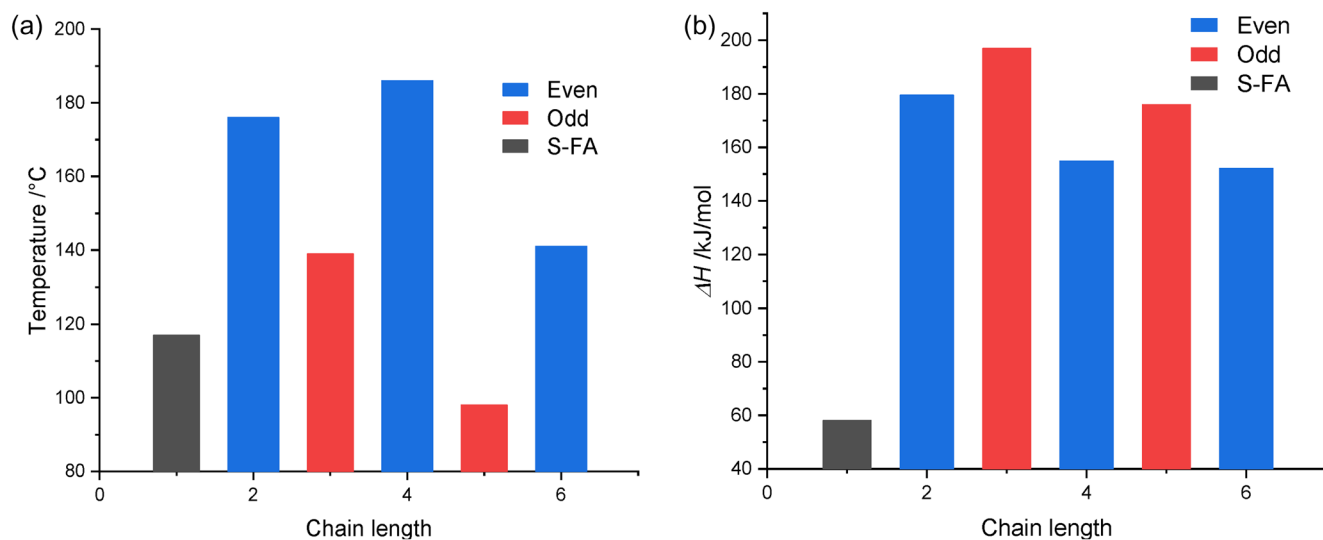
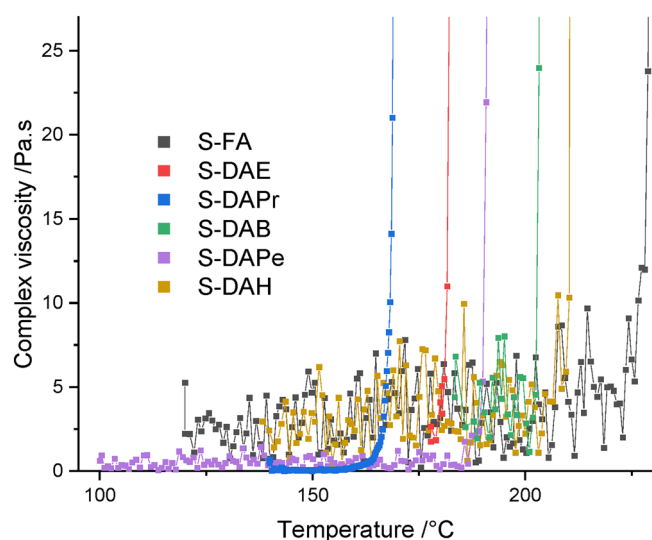


FIGURE 3 | Evolution of T_m (a) and ΔH (b) in dependency on the number of methylene groups in sesamol based benzoxazine monomers determined by DSC. [Color figure can be viewed at [wileyonlinelibrary.com](https://onlinelibrary.wiley.com)]

TABLE 1 | Thermal properties of sesamol based benzoxazines determined by DSC and rheology.

Sample	C atoms ^a	T_m (°C) ^b	T_{onset} (°C) ^c	T_p (°C) ^d	T_{onset} (°C) ^e	ΔH_M (kJ/mol)	$T_{manufacturing}$ (°C)
S-FA	0	117	227	234	230	58	130
S-DAE	2	176	187	196	185	180	$T_m > T_{manufacturing}$ ^f
S-DAPr	3	139	190	197	175	197	145
S-DAB	4	186	200	213	200	155	$T_m > T_{manufacturing}$ ^f
S-DAPe	5	98	214	224	195	176	105
S-DAH	6	141	218	226	210	152	145

^aNumber of C atoms in the linker chain.^bMelting point.^cPolymerization begin determined by DSC.^dPolymerization peak determined by DSC.^ePolymerization begin determined by increased viscosity above 15 Pas.^f T_m too high for $T_{manufacturing}$.**FIGURE 4** | Rheology in oscillating mode resulting complex viscosity in dependency of the temperature. [Color figure can be viewed at [wileyonlinelibrary.com](https://onlinelibrary.wiley.com)]

benzoxazines were significantly higher compared to S-FA which had a $T_{5\%}$ of 144°C. This higher thermal stability may be a result of the increased molecular size, which resulted in a reduced volatility.

All in all, thermal analyses revealed that all bifunctional benzoxazines had a thermal stability of at least 182°C. However, linker chain lengths on the one hand and an even or odd number of methylene groups on the other hand affected both melting point and T_{onset} of the ROP. Monomers with an odd numbered aliphatic linker had a lower T_m and an increased ΔH_M during polymerization in comparison to their even counterparts.

2.2.2 | Polymer Related Properties

Based on the obtained T_{onset} 's and $T_{5\%}$ of the monomers, sesamol based polymers pS-DAE, pS-DAPr, pS-DAB, pS-DAPe, pS-DAH, and pS-FA were obtained after curing at 200°C for

2h while applying a pressure of 15 bar in a microscopic scale. The diamine-based polybenzoxazines showed $T_{5\%}$ between 268°C for pS-DAPr and 290°C for pS-DAH under ambient atmosphere. However, no dependency on the chain lengths was found under both nitrogen (Figure 5a and Table S2) and ambient atmosphere (Figure 5b and Table S3). All bifunctional polybenzoxazines were less stable than the monofunctional pS-FA ($T_{5\%}$ of 310°C). At 800°C, pS-FA, pS-DAE, pS-DAPr, and pS-DAB revealed similar char yields in the range between 58% and 63%, whereas pS-DAPe and pS-DAH exhibited lower values around 51% under nitrogen atmosphere. Overall, a decreased thermal stability (Tables S2 and S3) and a lower char yield were observed for pS-DAPe and pS-DAH in comparison to pS-DAE, pS-DAPr, and pS-DAB which resulted from their higher aliphatic content and the subsequently reduced crosslinking density. A parity dependency was not found.

Additionally, combustion properties of sesamol-based polybenzoxazines were investigated by determining their temperature-dependent heat release via MCC analysis (Table 2). The peak heat release rate ($PHRR$), total heat release (THR) and the temperature at the $PHRR$ ($TPHRR$) increase with an increasing chain length for all bifunctional polybenzoxazines. Longer aliphatic chains lead to an increased fuel generation for the heat releasing combustion process during their thermal decomposition. Thus, for sesamol-based polymers the ratio of aromatic structure and methylene groups changes with an increasing aliphatic chain length shifting thermal properties to lower thermal stability and therefore a higher fuel generation. The effect can be best seen with the $PHRR$ which is double as high for pS-DAPe and pS-DAH than for the other bifunctional benzoxazines. As pS-FA contains the least aliphatic units, it exhibited the lowest THR with 3.0 kJ/g in comparison to 4.6 kJ/g for pS-DAE and 8.9 kJ/g for pS-DAH. Due to the high ΔH of S-DAPr it is expected that a partial degradation process starts during the polymerization, which lowers the amount of degradable material. Therefore, the overall value of the $PHRR$ and THR is slightly lower in comparison to the increasing chain length. Furthermore, the ignition Temperature (T_1) slightly increases with increasing chain length from 244°C for pS-DAE up to 255°C for pS-DAH. This trend is in accordance with the $T_{5\%}$ data of the polymers (Table S2).

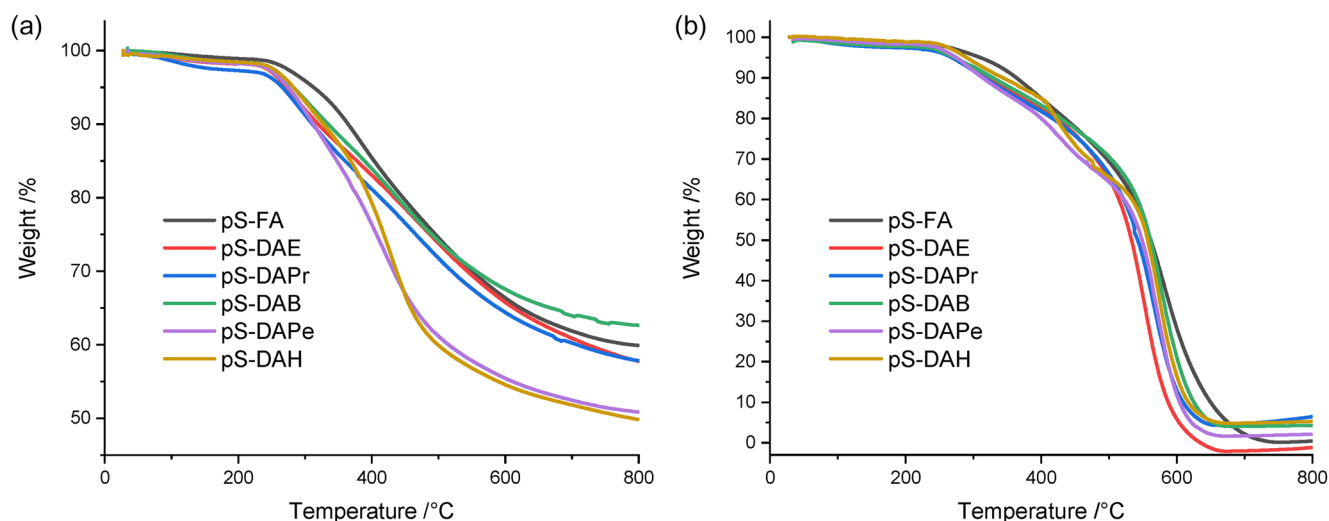


FIGURE 5 | TGA results of sesamol based polybenzoxazines with aliphatic diamines or furfurylamine under N_2 (a) and ambient atmosphere (b). [Color figure can be viewed at [wileyonlinelibrary.com](https://onlinelibrary.wiley.com)]

TABLE 2 | Results from micro cone calorimeter analysis from small scale polybenzoxazine samples.

Sample	PHRR _p (W/g)	TPHRR (°C)	THR (kJ/g)	Char yield (%)	T _I (°C)
pS-FA	8	575	3.0	60	165
pS-DAE	13	303	4.6	57	244
pS-DAPr	11	410	3.5	59	246
pS-DAB	17	399	5.6	53	251
pS-DAPe	41	419	8.9	48	250
pS-DAH	65	441	8.9	48	255

2.3 | Study of Manufacturing Parameters for Bifunctional Sesamol Benzoxazines

After analyzing the polybenzoxazines on a microscopic scale, macroscopic samples for DMA tests were manufactured next. For this, the monomers were molten and degassed at specific temperatures (Table 1 and Figure S5) for 30 min, before a temperature ramp was applied for polymerization. The degassing step was necessary to remove volatile components from the molten monomers and to avoid porous samples. However, for S-DAE, S-DAPr, and S-DAB a highly viscous foam formed during the degassing, which led to the formation of porous samples. This observation can be explained by an insufficient small temperature window between T_m and T_{onset} , which resulted in a rapidly increasing viscosity during the degassing step that could be observed during the curing. A similar finding was previously reported for a benzoxazine based on DAE and vanillin [7]. Therefore, only the pair of S-DAPe and S-DAH was chosen for the polymerization experiments, as their T_m 's were much lower than the other bifunctional monomers resulting in an adequate time frame for the degassing step. In the same way, S-FA also exhibited a sufficient time frame due to its low melting point and was polymerized macroscopically as well.

DMA samples of the three monomers were manufactured under the same polymerization conditions as the microscopic samples. The resulting polymers were homogeneous and without

macroscopic voids. However, S-FA samples were quite thin and had lost at least 50% of the monomer mass during the polymerization. Nonetheless, while obtaining polymer samples the combination of high temperature and pressure made the manufacturing of these materials challenging. Therefore, it was investigated if the application of pressure could be avoided by adjusting the polymerization conditions while still obtaining porous-free samples. Two different approaches were investigated to avoid the usage of pressure (P), namely lower polymerization temperatures (T) and the use of resorcinol as initiator (I). In the first attempt, it was tested if a significant lower polymerization temperature could avoid the formation of pores by having less decomposition products. Therefore, S-DAH, S-DAPe, and S-FA were polymerized at 155°C to avoid the decomposition at higher temperatures. Due to the lower polymerization temperature the polymerization time was increased to 24 h. However, neat samples could only be achieved for S-DAH. With pS-FA and pS-DAPe solid but highly porous and brittle samples were obtained. That can be explained with the low $T_{5\%}$ of 144°C and therefore earlier decomposition for S-FA. For S-DAPe the higher ΔH in comparison to S-DAH probably resulted in higher polymerization temperatures in the bulk which then led to a decomposition of the monomer. In the second attempt, S-DAH was mixed with 5 mol% of resorcinol as initiator to decrease the initial polymerization temperature below the decomposition temperatures of S-DAH and S-DAPe and to increase the polymerization speed to avoid pore formation. It could be shown that a content of

TABLE 3 | DMA results for sesamol based polybenzoxazines either thermally induced at with additional pressure (P), ambient atmosphere (T), or with resorcinol as initiator (I).

Sample	E' @25°C (GPa)	T_g (°C) ^a
pS-DAH 200-P	2.1	231
pS-DAH 155-T	1.5	177
pS-DAH 160-I	0.6	164
pS-DAH 170-I	0.7	172
pS-DAH 180-I	0.9	176
pS-DAP 200-P	2.4	228
pS-FA 200-P	0.8	220

^a T_g was determined by the maximum of the loss modulus.

5 mol% resorcinol decreased T_{onset} , for example, for S-DAH, by almost 20°C to 200°C while it did not reduce the initial degradation temperature significantly from 191°C to 187°C (Table S4 and Figure S6). For S-DAH, initiator containing samples could be polymerized porous-free at 160°C, 170°C and 180°. However, the same study was performed for S-FA and S-DAPe, which led again to porous and brittle samples, as the polymerization temperatures still were too high in comparison to the $T_{5\%}$ and for S-DAPe the initiator accelerated the polymerization and therefore, led to a higher energy release. However, a higher initiator concentration would decrease the decomposition temperature of S-FA further and also accelerate the polymerization for S-DAPe, causing the same problems as already describes earlier. These results indicated that the monomer decomposition and pore formation were inevitable for S-FA and S-DAPe during curing without pressure.

In summary, all three methods could be used to obtain non-porous polymers from S-DAH, whereas for S-DAPe and S-FA only an increased pressure approach resulted in non-porous polymers.

DMA samples obtained from the various polymerization conditions were analyzed in the temperature range of 0°C–250°C (Table 3 and Figure S7). The following storage moduli were measured at 25°C and the stated temperatures are based on the respective polymerization procedure. The polymers resulting from resorcinol mediated polymerization of S-DAH revealed the overall lowest storage modulus of 0.6 GPa, which slightly increased to 0.9 GPa with increasing polymerization temperature. The increasing temperature increased the conversion of S-DAH based monomers and led to higher E' . Nevertheless, the overall presence of resorcinol inside the network may seem to cause a decrease of the cross-linking density compared to the other curing methods. Interestingly, a significantly higher E' of 1.5 GPa was obtained for S-DAH after polymerization at 155°C for 24 h, revealing that this approach was an attractive alternative in comparison to the use of initiators. Potentially, the lower polymerization temperature and the longer polymerization time led to less defects and a thorough polymerization. However, the highest storage modulus was achieved by the combination of high polymerization temperature and increased pressure resulting in a E' of 2.1 GPa for pS-DAH. The slightly higher temperatures

and especially the additional pressure likely increased the network density even further and reduced the size of potential defects, resulting in the overall highest E' of all S-DAH samples.

A slightly higher E' of 2.4 GPa was found for pS-DAPe polymerized under pressure. This was probably a result of the higher crosslinking density due to the shorter aliphatic chain compared to pS-DAH. In contrast, the monofunctional character of pS-FA resulted in a lower crosslinking density and therefore, in a significantly lower E' of 0.8 GPa.

In addition to the storage modulus, the glass transition temperature (T_g) was also determined from the DMA results (Table 3). A similar trend as for E' was seen for pS-DAH. Samples polymerized with 5 mol% resorcinol exhibited the overall lowest T_g whereas the polymerization at 155°C for 24 h revealed a slightly higher T_g of 177°C. The highest T_g of 231°C was obtained for pS-DAH polymerized at 15 bar and 200°C. Furthermore, the polymerization process under pressure did not reveal a significant influence of the aliphatic chain length on the T_g of the successfully polymerized monomers as pS-DAPe had a similar T_g of 228°C. However, the lower T_g of pS-FA around 220°C indicated that bifunctional monomers yield slightly higher T_g due to their higher crosslinking density in comparison to pS-FA, similar to the E' results. In comparison to previously reported T_g for sesamol- and polyethyleneimine based benzoxazines (149°C) [23] or sesamol-, furfurylamine- and benzaldehyde-based benzoxazines (165°C) [21] sesamol-based benzoxazines containing aliphatic amines showed a significantly higher T_g . Furthermore, sesamol proves to be a promising biobased substitute for conventional phenolic components as the resulting polymer pS-DAH exhibited a T_g higher than for benzoxazines based on DAH with phenol (169°C), o-Cresol (121°C), or p-Cresol (145°C) instead of sesamol [32].

All in all, the E' moduli and T_g results indicated that a lower polymerization temperature in combination with a longer polymerization time could be an alternative to an initiator-based polymerization of bio-based benzoxazine monomers because degradation processes are avoided. However, curing processes under additional pressure are still necessary to maximize the T_g as well as for monomers with a low thermal stability. Furthermore, the shorter aliphatic chain length of pS-DAPe had only a minor impact on E' and T_g compared to pS-DAH. In addition, upon exceeding the T_g all samples broke in the DMA experiments. The $T_{5\%}$ above 260°C indicated that the breakage was a result of the expansion from microscopic voids and not a thermal degradation. A general trend for the influence of the aliphatic chain length on the thermo-mechanical properties could not be determined due to the missing DMA data for pS-DAE, pS-DAPr, and pS-DAB, but would be expected. With increasing chain length, the crosslinking density should decrease as the distance between network points increases. The lowering crosslinking density would then reduce E' and T_g for increasing chain lengths [31, 32].

3 | Conclusion

Bisbenzoxazines based on sesamol and aliphatic diamines, namely S-DAE, S-DAPr, S-DAB, S-DAPe, and S-DAH, have

been synthesized successfully following the Green Chemistry approaches by using ethanol as green solvent except for S-DAPr.

A systematic variation in chain length of the aliphatic diamine linker proved a parity effect with respect to the thermal properties. The melting temperature of even numbered aliphatic linkers in bisbenzoxazines such as in S-DAE ($T_m = 176^\circ\text{C}$) and S-DAB ($T_m = 186^\circ\text{C}$) was exceptionally high compared to odd numbered linkers such as in S-DAPr ($T_m = 139^\circ\text{C}$) and S-DAPE ($T_m = 98$). This is in agreement with reported parity dependencies for other polymers and indicates that for molecules with an odd number of methylene groups in the linker the symmetry seem to be reduced which affects the melting behavior. S-DAPE revealed the lowest T_m of 98°C while S-DAE and S-DAB exhibited a high T_m of 176°C and 186°C , respectively. Analysis of the monomer's thermal stability revealed that S-FA started to degrade at 144°C , whereas bifunctional sesamol-based monomers were stable at least until 182°C . The polymerization behavior was investigated by T_{onset} determinations showing a general increase of T_{onset} with longer aliphatic chain length. In combination with the high T_m the polymerization of S-DAE, S-DAPr, and S-DAB is restricted. Therefore, only S-DAPE, S-DAH, and S-FA have been polymerized either under pressure, longer polymerization time or mediated by resorcinol yielding samples for thermo-mechanical analysis. Polymerizations performed with additional pressure led to polymers with astonishing high T_g of more than 228°C and an E' up to 2.4 GPa for pS-DAP. In comparison to previously reported T_g for sesamol- and polyethyleneimine based benzoxazines or sesamol-, furfurylamine- and benzaldehyde-based benzoxazines sesamol-based benzoxazines containing aliphatic amines showed a significantly higher T_g .

First degradation started around 265°C for all polymers, which were polymerized at 200°C with 15 bar pressure. The char yield was above 58% for shorter aliphatic chains and 51% for S-DAPE and S-DAH. Furthermore, MCC analysis from sesamol based polymers revealed both an increasing PHRR and an increasing T_i with a longer aliphatic chain and therefore, indicating a slight influence of the chain length on the thermal properties.

Overall, the sesamol-based monomers with DAPE and DAH exhibited high thermo-mechanical properties and a high thermal stability in comparison to benzoxazines based on conventional phenolic components. With respect to the molecular design one should take into account the huge effect of marginal changes in the number of methylene groups as well the parity of an aliphatic linker on the thermal and thermo-mechanical behavior.

4 | Experimental Section and Methods

4.1 | Materials and Reagents

Diaminoethane (DAE, 99%), diaminopropane (DAPr, 98%), diaminobutane (DAB, 99%), diaminohexane (DAH, 98%), ethanol, and paraformaldehyde (crystalline) were obtained from Sigma Aldrich (Taufkirchen, Germany). Sesamol (S, 98%) and

furfuryl amine (FA, 99%) were supplied from abcr (Karlsruhe, Germany). Diaminopentane (DAPE, 98%) was supplied from TCI (Zwijndrecht, Belgium). Magnesium sulfate and chloroform were obtained from Carl Roth (Karlsruhe, Germany). All chemicals were used without further purification. Sesamol and furfuryl amine based benzoxazine (S-FA) was synthesized as previously described [14].

4.2 | Synthesis Procedures

The following synthesis procedure was applied to DAE, DAB and DAH with the same equivalents only altered by molar mass of diamine. Sesamol (4.00 g, 14.5 mmol, 2 Eq), paraformaldehyde (0.880 g, 29.3 mmol, 4.05 Eq) and diamine (e.g., for DAH 0.841 g, 7.24 mmol, 1 Eq) were mixed in ethanol (25 mL). The mixture was heated to 78°C for 2 h. All reactants were dissolved before the crude product precipitated. The crude product was filtered, washed three times with ethanol (75 mL) and dried in a vacuum oven for 14 h at 80°C .

4.2.1 | Sesamol/Diaminoethane-Based Benzoxazine Monomer (S-DAE)

1,2-bis(6H-[1,3]dioxolo[4',5':4,5]benzo[1,2-e][1,3]oxazin-7(8H)-yl)ethane was synthesized according to the above procedure and obtained as white powder in a 75% yield (Figure S8).

^1H NMR (CDCl_3 , 600 MHz, 298 K): δ (ppm) = (assignment, multiplicity, experimental integration, and theoretical integration). $\delta = 6.40$ (Ar-H, s, exp. 2.00H, th 2.00H); 6.34 (Ar-H, s, exp. 1.85H, th 2.00H); 5.86 (O-CH₂-O, s, exp. 4.00H, th 4.00H); 4.81 (N-CH₂-O, s, exp. 4.07H, th 4.00H); 3.93 (Ar-CH₂-N, s, exp. 4.12H, th 4.00H); 2.94 (N-CH₂-N, s, exp. 4.21H, th 4.00H) ppm; ^{13}C NMR (CDCl_3 , 600 MHz, 298 K): δ (ppm) = (assignment). $\delta = 148$ (H); 146 (F); 141 (E); 112 (I); 106 (D); 100 (A); 98 (G); 82 (B); 50 (L); 49 (C) ppm; MS (EI) m/z for $\text{C}_{20}\text{H}_{20}\text{N}_2\text{O}_6$ was 384.13341.

4.2.2 | Sesamol/Diaminobutane-Based Benzoxazine Monomer (S-DAB)

1,4-bis(6H-[1,3]dioxolo[4',5':4,5]benzo[1,2-e][1,3]oxazin-7(8H)-yl)butane was synthesized as according to the above procedure and obtained as white powder in a 71% yield.

^1H NMR (CDCl_3 , 600 MHz, 298 K): δ (ppm) = (assignment, multiplicity, experimental integration, and theoretical integration). $\delta = 6.40$ (Ar-H, s, exp. 2.16H, th 2.00H); 6.33 (Ar-H, s, exp. 1.91H, th 2.00H); 5.86 (O-CH₂-O, s, exp. 4.00H, th 4.00H); 4.77 (N-CH₂-O, s, exp. 3.90H, th 4.00H); 3.87 (Ar-CH₂-N, s, exp. 4.04H, th 4.00H); 2.74 (N-CH₂-CH₂, t, exp. 3.97H, th 4.00H); 1.59 (N-CH₂-CH₂, p, exp. 4.77, th 4.00) ppm; ^{13}C NMR (CDCl_3 , 600 MHz, 298 K): δ (ppm) = (assignment). $\delta = 148$ (H); 146 (F); 141 (E); 112 (I); 106 (D); 100 (A); 98 (G); 82 (B); 51 (C); 50 (L); 26 (M) ppm; MS (EI) m/z for $\text{C}_{22}\text{H}_{24}\text{N}_2\text{O}_6$ was 412.16395.

4.2.3 | Sesamol/Diaminohexane-Based Benzoxazine Monomer (S-DAH)

1,6-bis(6H-[1,3]dioxolo[4',5':4,5]benzo[1,2-e][1,3]oxazin-7(8H)-yl)hexane was synthesized according to the above procedure and obtained as white powder in a 76% yield.

^1H NMR (CDCl_3 , 600 MHz, 298 K): δ (ppm) = (assignment, multiplicity, experimental integration, theoretical integration). δ = 6.40 (Ar-H, s, exp. 2.01H, th 2.00H); 6.33 (Ar-H, s, exp. 1.80H, th 2.00H); 5.86 (O- CH_2 -O, s, exp. 4.00H, th 4.00H); 4.77 (N- CH_2 -O, s, exp. 4.05H, th 4.00H); 3.87 (Ar- CH_2 -N, s, exp. 4.01H, th 4.00H); 2.70 (N- CH_2 - CH_2 , t, exp. 4.20H, th 4.00H); 1.54 (N- CH_2 - CH_2 , p, exp. 4.52, th 4.00); 1.35 (N- CH_2 - CH_2 , p, exp. 3.96, th 4.00) ppm; ^{13}C NMR (CDCl_3 , 600 MHz, 298 K): δ (ppm) = (assignment). δ = 148 (H); 146 (F); 141 (E); 112 (I); 106 (D); 100 (A); 98 (G); 82 (B); 51 (C); 50 (L); 28 (M); 27 (N) ppm; MS (EI) m/z for $\text{C}_{24}\text{H}_{28}\text{N}_2\text{O}_6$ was 440.19522.

4.2.4 | Sesamol/Diaminopentane-Based Benzoxazine Monomer (S-DAPe)

1,5-bis(6H-[1,3]dioxolo[4',5':4,5]benzo[1,2-e][1,3]oxazin-7(8H)-yl)pentane was synthesized in an altered way. Sesamol (4.00 g, 14.5 mmol, 2.00 Eq), paraformaldehyde (0.880 g, 29.3 mmol, 4.05 Eq) and DAPe (0.739 g, 7.24 mmol 1.00 Eq) were mixed in ethanol (25 mL). The mixture was heated to 78°C for 2 h. All reactants were dissolved until a brownish oil formed. The mixture was allowed to cool down to 25°C, ethanol and side products were decanted. Ethanol (15 mL) was added and the mixture was heated to 78°C again. Afterwards, the mixture was poured into a large beaker and the crude product precipitated for 48 h, filtered, washed three times with ethanol (75 mL) and dried in a vacuum oven for 24 h at 45°C. The product was obtained as off-white solid (69% yield).

^1H NMR (CDCl_3 , 600 MHz, 298 K): δ (ppm) = (assignment, multiplicity, experimental integration, and theoretical integration). δ = 6.40 (Ar-H, s, exp. 1.92H, th 2.00H); 6.33 (Ar-H, s, exp. 1.75H, th 2.00H); 5.85 (O- CH_2 -O, s, exp. 4.00H, th 4.00H); 4.76 (N- CH_2 -O, s, exp. 3.94H, th 4.00H); 3.87 (Ar- CH_2 -N, s, exp. 3.94H, th 4.00H); 2.71 (N- CH_2 - CH_2 , t, exp. 3.94H, th 4.00H); 1.57 (N- CH_2 - CH_2 , p, exp. 4.10, th 4.00), 1.37 (N- CH_2 - CH_2 , p, exp. 2.10, th 2.00) ppm; ^{13}C NMR (CDCl_3 , 600 MHz, 298 K): δ (ppm) = (assignment). δ = 148 (H); 146 (F); 141 (E); 112 (I); 106 (D); 100 (A); 98 (G); 82 (B); 51 (C); 50 (L); 28 (M); 25 (N) ppm; MS (EI) m/z for $\text{C}_{23}\text{H}_{26}\text{N}_2\text{O}_6$ was 426.17895.

4.2.5 | Sesamol/Diaminopropane-Based Benzoxazine Monomer (S-DAPr)

For the synthesis of 1,3-bis(6H-[1,3]dioxolo[4',5':4,5]benzo[1,2-e][1,3]oxazin-7(8H)-yl)propane, sesamol (2.00 g, 14.5 mmol, 2.00 Eq), paraformaldehyde (0.880 g, 29.3 mmol, 4.05 Eq) and DAPr (0.538 g, 7.24 mmol, 1.00 Eq) were dissolved in CHCl_3 (50 mL) and heated to 62°C for 24 h. The conversion was monitored by ^1H -NMR in CDCl_3 . In a separation funnel, the organic

layer was washed twice with sodium hydroxide (1 M), water, saturated sodium bicarbonate solution and brine. The organic layer was dried with magnesium sulfate and filtered before chloroform was removed under reduced pressure yielding a yellowish oil. The crude product crystallized over 48 h and washed three times with ethanol before drying for 14 h at 50°C. The product was obtained as grayish powder in low yield of 7%.

^1H NMR (CDCl_3 , 600 MHz, 298 K): δ (ppm) = (assignment, multiplicity, experimental integration, theoretical integration). δ = 6.40 (Ar-H, s, exp. 1.63H, th 2.00H); 6.33 (Ar-H, s, exp. 1.55H, th 2.00H); 5.85 (O- CH_2 -O, s, exp. 4.00H, th 4.00H); 4.76 (N- CH_2 -O, s, exp. 3.60H, th 4.00H); 3.88 (Ar- CH_2 -N, s, exp. 3.61H, th 4.00H); 2.79 (N- CH_2 - CH_2 , s, exp. 3.49H, th 4.00H); 1.78 (N- CH_2 - CH_2 , p, exp. 2.12, th 2) ppm; ^{13}C NMR (CDCl_3 , 600 MHz, 298 K): δ (ppm) = (assignment). δ = 148 (H); 146 (F); 141 (E); 112 (I); 106 (D); 100 (A); 98 (G); 82 (B); 50 (L); 49 (C); 27 (M) ppm; MS (EI) m/z for $\text{C}_{21}\text{H}_{22}\text{N}_2\text{O}_6$ found 398.14870.

4.3 | Benzoxazine Polymerization Procedure for Sample Manufacturing

Small scale polymer samples were prepared by weighing 50 mg of sesamol and diamine-based monomers into aluminum molds. The monomers were polymerized for 2 h at 180°C followed by 2 h at 200°C with a pressure of 15 bar.

Around 2 g of sesamol and diamine-based monomers were molten in a convection oven at selected temperatures, shortly stirred by hand and degassed for at least 15 min before transferring into a silica mold with dimensions of $35 \times 10 \times \text{mm}^3$ for one DMA test specimen. Different curing parameters were used: S-FA, S-DAH and S-DAPe were polymerized with a pressure of 15 bar in an autoclave and either for 3 h at 170°C, 2 h at 180°C and 2 h at 200°C or for 2 h 160°C, 2 h at 170°C and 4 h at 180°C. Heating ramps were 5 K/min until the first plateau of 170°C or 160°C was reached, the heating ramp to the second and third plateau was 2 K/min. In another attempt, S-Fa, S-DAH, and S-DAPe were polymerized at 155°C for 24 h without pressure.

4.4 | Analytical Methods for Characterization

FT-IR spectra were recorded on an Equinox 55 ATR spectrometer (Bruker, Bremen, Germany) in attenuated total reflection (ATR) mode using a diamond crystal with 32 scans from 650 to 4000 cm^{-1} and a resolution of 4 cm^{-1} .

^1H NMR spectra were recorded on an AVANCE NEO 600 MHz NMR-spectrometer (Bruker, Bremen, Germany) with CDCl_3 as solvent at 20°C. ^{13}C NMR spectra were recorded with a frequency of 150 MHz using the same spectrometer, pulse programs were zg_1H and zg_13C. The chemical shifts were reported in parts per million (ppm) and referred to residual CHCl_3 protons in the CDCl_3 .

HR-MS analysis were conducted using a Finnigan MAT 95XL mass spectrometer (Thermo Fisher Scientific, Bremen, Germany) via direct inlet mode with electron impact (EI) as ionization source and an electron energy of 70 eV.

Differential Scanning Calorimetry measurements were performed using a Discovery DSC (TA Instruments, Hüllhorst, Germany) with 10K/min in a range from 0°C to 300°C on a specimen scale of 1–2 mg under N₂ atmosphere in closed aluminum pans. All samples were measured in triple determination and the average values were used for the evaluation.

Rheological analyses were performed on an Advanced Rheometric Expansion system (TA Instruments, Hüllhorst, Germany) with a shear frequency of 25 Hz, a plate diameter of 25 mm and a gap of 0.2 mm in oscillatory mode either in a temperature range from 90°C to 220°C with a heating rate of 5 K/min to determine the temperature-dependent viscosity or isothermal at chosen temperatures to determine the pot-life.

DMA experiments were performed using the Dynamic Mechanical Analyzer Q800 (TA Instruments, Hüllhorst, Germany). Thermo-mechanical properties were determined in a temperature range from 0°C to 250°C with a heating rate of 2 K/min and a frequency of 1 Hz in a single cantilever bending mode, using a test specimen of 35 × 10 × 4 mm. The glass transition temperature (T_g) was determined by the maximum of loss modulus.

TGA measurements were carried out with a Q5000 (TA Instruments, Hüllhorst, Germany) in a temperature range from 25°C to 800°C and a heating rate of 10 K/min under both ambient or nitrogen atmosphere with a sample size of 1–2 mg for monomer and polymer samples.

MCC measurements were performed on a FAA micro combustion calorimeter (Fire Testing Technology, East Grinstead, UK) according to ASTM D7309 in a temperature range from 75°C to 1000°C with a heating rate of 1 K/s. The resulting data was fitted using software from the same manufacturer to determine peak heat release rate (*PHRR*), temperature at the peak heat release rate (*TPHRR*) and total heat release (*THR*). In addition, the onset of the first heat release rate (*HRR*) maximum was defined as ignition temperature (T_i). Charr yields were determined by weighing and comparing the sample masses before and after the measurement.

Author Contributions

Thorben S. Haubold: investigation (lead), validation (lead), visualization (lead), writing – original draft (lead). **Gideon Abels:** conceptualization (supporting), data curation (supporting), investigation (equal), validation (supporting), writing – review and editing (equal). **Katharina Koschek:** funding acquisition (lead), project administration (lead), resources (lead), supervision (equal), writing – review and editing (equal).

Acknowledgments

The authors gratefully acknowledge the financial support from the Bundesministerium für Wirtschaft und Klima (BMWK) (GreenLight, 03SX515E). Open Access funding enabled and organized by Projekt DEAL.

Conflicts of Interest

The authors declare no conflicts of interest.

Data Availability Statement

The data that support the findings of this study are available on request from the corresponding author upon reasonable request.

References

1. H. Ishida and H. Y. Low, “A Study on the Volumetric Expansion of Benzoxazine-Based Phenolic Resin,” *Macromolecules* 30 (1997): 1099–1106.
2. C. Jubsilp, T. Takeichi, and S. Rimdusit, “Effect of Novel Benzoxazine Reactive Diluent on Processability and Thermomechanical Characteristics of Bi-Functional Polybenzoxazine,” *Journal of Applied Polymer Science* 104 (2007): 2928–2938.
3. H. Ishida and D. P. Sanders, “Improved Thermal and Mechanical Properties of Polybenzoxazines Based on Alkyl-Substituted Aromatic Amines,” *Journal of Polymer Science Part B: Polymer Physics* 38 (2000): 3289–3301.
4. R. Andreu, M. A. Espinosa, M. Galià, V. Cádiz, J. C. Ronda, and J. A. Reina, “Synthesis of Novel Benzoxazines Containing Glycidyl Groups: A Study of the Crosslinking Behavior,” *Journal of Polymer Science Part A: Polymer Chemistry* 44 (2006): 1529–1540.
5. N. Amarnath, D. Appavoo, and B. Lochab, “Eco-Friendly Halogen-Free Flame Retardant Cardanol Polyphosphazene Polybenzoxazine Networks,” *ACS Sustainable Chemistry & Engineering* 6 (2017): 389–402.
6. R. Ganfoud, N. Guigo, L. Puchot, P. Verge, and N. Sbirrazzuoli, “Investigation on the Role of the Alkyl Side Chain of Cardanol on Benzoxazine Polymerization and Polymer Properties,” *European Polymer Journal* 119 (2019): 120–129.
7. L. Puchot, P. Verge, T. Fouquet, C. Vancaeyzeele, F. Vidal, and Y. Habibi, “Breaking the Symmetry of Dibenzoxazines: A Paradigm to Tailor the Design of Bio-Based Thermosets,” *Green Chemistry* 18 (2016): 3346–3353.
8. C. Wang, J. Sun, X. Liu, A. Sudo, and T. Endo, “Synthesis and Copolymerization of Fully Bio-Based Benzoxazines From Guaiacol, Furfurylamine and Stearylamine,” *Green Chemistry* 14 (2012): 2799.
9. R. Yang, M. Han, B. Hao, and K. Zhang, “Biobased High-Performance Tri-Furan Functional Bis-Benzoxazine Resin Derived From Renewable Guaiacol, Furfural and Furfurylamine,” *European Polymer Journal* 131 (2020): 109706.
10. N. Teng, S. Yang, J. Dai, et al., “Making Benzoxazine Greener and Stronger: Renewable Resource, Microwave Irradiation, Green Solvent, and Excellent Thermal Properties,” *ACS Sustainable Chemistry & Engineering* 7, no. 9 (2019): 8715–8723.
11. L. Dumas, L. Bonnaud, M. Olivier, M. Poorteman, and P. Dubois, “Bio-Based High Performance Thermosets: Stabilization and Reinforcement of Eugenol-Based Benzoxazine Networks With BMI and CNT,” *European Polymer Journal* 67 (2015): 494–502.
12. A. Trejo-Machin, P. Verge, L. Puchot, and R. Quintana, “Phloretic Acid as an Alternative to the Phenolation of Aliphatic Hydroxyls for the Elaboration of Polybenzoxazine,” *Green Chemistry* 19 (2017): 5065–5073.
13. A. Adjaoud, L. Puchot, C. E. Federico, R. Das, and P. Verge, “Lignin-Based Benzoxazines: A Tunable Key-Precursor for the Design of Hydrophobic Coatings, Fire Resistant Materials and Catalyst-Free Vitrimers,” *Chemical Engineering Journal* 453 (2023): 139895.
14. M. L. Salum, D. Iguchi, C. R. Arza, L. Han, H. Ishida, and P. Froimowicz, “Making Benzoxazines Greener: Design, Synthesis, and Polymerization of a Biobased Benzoxazine Fulfilling Two Principles of Green Chemistry,” *ACS Sustainable Chemistry & Engineering* 6 (2018): 13096–13106.

15. X. Wang, H. Niu, J. Huang, L. Song, and Y. Hu, "A Desoxyanisoin- and Furfurylamine-Derived High-Performance Benzoxazine Thermoset With High Glass Transition Temperature and Excellent Anti-Flammability," *Polymer Degradation and Stability* 189 (2021): 109604.
16. M. Monisha, N. Yadav, and B. Lochab, "Sustainable Framework of Chitosan–Benzoxazine With Mutual Benefits: Low Curing Temperature and Improved Thermal and Mechanical Properties," *ACS Sustainable Chemistry & Engineering* 7 (2019): 4473–4485.
17. N. Amarnath, S. Shukla, and B. Lochab, "Isomannide-Derived Chiral Rigid Fully Biobased Polybenzoxazines," *ACS Sustainable Chemistry & Engineering* 7 (2019): 18700–18710.
18. R. Tavernier, L. Granado, G. Foyer, G. David, and S. Caillol, "Formaldehyde-Free Polybenzoxazines for High Performance Thermosets," *Macromolecules* 53 (2020): 2557–2567.
19. S. F. Li and W. D. Huang, "Synthesis of New Benzoxazine From Cardanol-Furfural Resin and the Properties of the Corresponding Polymer," *Advanced Materials Research* 236-238 (2011): 317–320.
20. Y. Lyu and H. Ishida, "Natural-Sourced Benzoxazine Resins, Homopolymers, Blends and Composites: A Review of Their Synthesis, Manufacturing and Applications," *Progress in Polymer Science* 99 (2019): 101168.
21. I. Machado, I. Hsieh, E. Rachita, et al., "A Truly Bio-Based Benzoxazine Derived From Three Natural Reactants Obtained Under Environmentally Friendly Conditions and Its Polymer Properties," *Green Chemistry* 23 (2021): 4051–4064.
22. H. Liu, S. Li, Z. Zhang, B. Li, and M. Xu, "An Efficient and Convenient Strategy Toward Fire Safety and Water Resistance of Polypropylene Composites Through Design and Synthesis of a Novel Mono-Component Intumescent Flame Retardant," *Polymers for Advanced Technologies* 26 (2019): 5.
23. M. Necolau, I. E. Biru, J. Ghițman, C. Stavarache, and H. Iovu, "Insightful Characterization of Sesamol-Based Polybenzoxazines: Effect of Phenol and Amine Chain Type on Physical and Nanomechanical Properties," *Polymer Testing* 110 (2022): 107578.
24. K. Thongbhubate, K. Irie, Y. Sakai, A. Itoh, and H. Suzuki, "Improvement of Putrescine Production Through the Arginine Decarboxylase Pathway in *Escherichia coli* K-12," *AMB Express* 11 (2021): 168.
25. M. J. Burk, A. P. Burgard, R. E. Osterhout, and P. Pharkya, "Genomatica Inc," *EP3611254A1*, (2020).
26. S. Bunsupa, M. Yamazaki, and K. Saito, "Quinolizidine Alkaloid Biosynthesis: Recent Advances and Future Prospects," *Frontiers in Plant Science* 3 (2012): 239.
27. C. W. Bunn, "The Melting Points of Chain Polymers," *Journal of Polymer Science Part B: Polymer Physics* 34 (1996): 799–819.
28. R. Boese, H.-C. Weiss, and D. Bläser, "The Melting Point Alternation in the Short-Chainn-Alkanes: Single-Crystal X-Ray Analyses of Propane at 30 K and of n-Butane Ton-Nonane at 90 K," *Angewandte Chemie, International Edition* 38 (1999): 988–992.
29. R. A. Pérez-Camargo, L. Meabe, G. Liu, et al., "Even–Odd Effect in Aliphatic Polycarbonates With Different Chain Lengths: From Poly (Hexamethylene Carbonate) to Poly (Dodecamethylene Carbonate)," *Macromolecules* 54 (2021): 259–271.
30. C. Zhou, Z. Wei, Y. Yu, et al., "Biobased Long-Chain Aliphatic Polyesters of 1,12-Dodecanedioic Acid With a Variety of Diols: Odd-Even Effect and Mechanical Properties," *Materials Today Communications* 19 (2019): 450–458.
31. D. J. Allen and H. Ishida, "Polymerization of Linear Aliphatic Diamine-Based Benzoxazine Resins Under Inert and Oxidative Environments," *Polymer* 48 (2007): 6763–6772.
32. D. J. Allen and H. Ishida, "Effect of Phenol Substitution on the Network Structure and Properties of Linear Aliphatic Diamine-Based Benzoxazines," *Polymer* 50 (2009): 613–626.

Supporting Information

Additional supporting information can be found online in the Supporting Information section.